Safety and Efficacy of *Para*-Aminohippurate Coinfusion for Renal Protection During Peptide Receptor Radiotherapy in Patients with Neuroendocrine Tumors

Alexandros Moraitis[1,2], Walter Jentzen[1,2], Pedro Fragoso Costa[1,2], David Kersting[1,2], Stephan Himmen[1,2], Marta Coelho[1,2], Marian Meckel[3], Cees J.A. van Echteld[4], Wolfgang P. Fendler[1,2], Ken Herrmann[1,2], and Miriam Sraieb[1,2]

[1]*Department of Nuclear Medicine, West German Cancer Center, University Hospital Essen, University of Duisburg-Essen, Essen, Germany;* [2]*German Cancer Consortium, Partner Site University Hospital Essen, Essen, Germany;* [3]*ITM Isotope Technologies Munich SE, Garching/Munich, Germany; and* [4]*Helacor Consultancy, Oberwil, Switzerland*

Para-aminohippurate, also known as *p*-aminohippuric acid (PAH), is used clinically to measure effective renal plasma flow. Preclinically, it was shown to reduce ^{177}Lu-DOTATOC uptake in the kidneys while improving bioavailability compared with amino acid (AA) coinfusion. We report the safety and efficacy of PAH coinfusion during peptide receptor radiotherapy in patients with neuroendocrine tumors. **Methods:** Twelve patients with metastatic or unresectable gastroenteropancreatic neuroendocrine tumors received ^{177}Lu-DOTATOC in 33 treatment cycles. Either 8 g of PAH or a mixture of 25 g of arginine and 25 g of lysine were coinfused. Safety was assessed by monitoring laboratory data, including hematologic and renal data, as well as electrolytes obtained before and 24 h after treatment. For radiation dosimetry, whole-body scans were performed at 1, 24, and 48 h and a SPECT/CT scan was performed at 48 h, along with blood sampling at 5 min and 0.5, 2, 4, 24, and 48 h after administration. Absorbed dose estimations for the kidneys and bone marrow were performed according to the MIRD concept. **Results:** In 15 treatment cycles, PAH was coinfused. No changes in mean creatinine level, glomerular filtration rate, and serum electrolytes were observed before or 24 h after treatment when using PAH protection ($P \geq 0.20$), whereas serum chloride and serum phosphate increased significantly under AA (both $P < 0.01$). Kidney–absorbed dose coefficients were 0.60 ± 0.14 Gy/GBq with PAH and 0.53 ± 0.16 Gy/GBq with AA. Based on extrapolated cumulative kidney-absorbed doses for 4 cycles, 1 patient with PAH protection and 1 patient with AA protection in our patient group would exceed the 23-Gy conservative threshold. The bone marrow–absorbed dose coefficient was 0.012 ± 0.004 Gy/GBq with PAH and 0.012 ± 0.003 Gy/GBq with AA. **Conclusion:** PAH is a promising alternative to AA for renal protection during peptide receptor radiotherapy. Further research is required to systematically investigate the safety profile and radiation dosimetry at varying PAH plasma concentrations.

Key Words: dosimetry; NET; PAH; PRRT; renal protection

J Nucl Med 2024; 65:931–937
DOI: 10.2967/jnumed.123.266619

Neuroendocrine tumors (NETs) represent a heterogeneous group of neoplasms and arise in various organs, mostly the gastrointestinal tract but also the pancreas and lungs. For metastatic disease, 5-y survival is reported to be less than 50%, which poses the need for adequate treatment options (*1*). Subsequent to the results of the NETTER-I trial, peptide receptor radiotherapy (PRRT) using ^{177}Lu-DOTA ligands coupled to somatostatin analogs has evolved into a valuable strategy for patients with unresectable or metastatic NETs (*2*).

In extensively treated NET patients, hematopoietic or renal toxicity are the dose-limiting morbidities in PRRT. Although bone marrow is typically not the dose-limiting organ, grade 3 or 4 hematologic toxicity, according to the Common Terminology Criteria for Adverse Events (National Cancer Institute), has been reported in approximately 10% of patients after PRRT (*3*,*4*). Radiolabeled peptides undergo renal clearance with active retention or reabsorption by the renal proximal tubular cells. High and prolonged renal uptake may lead to radiation-induced acute chronic nephrotoxicity that can significantly affect quality of life and long-term outcomes. Consequently, in PRRT, the kidney-absorbed dose is considered one of the major dose-limiting factors (*5*,*6*).

The kidney-absorbed dose can be reduced by coinfusing agents that competitively inhibit reabsorption of radiolabeled compounds, such as positively charged amino acids (AAs), gelofusine, trypsinized albumin, or bovine serum albumin fragmented by cyanogen bromide (*5*,*7*–*9*). When using AA, an average reduction of absorbed dose in or uptake to the kidneys of between 23% and 47% was achieved compared with no renal protection (*8*,*10*,*11*). Although these data rely on a limited number of patients and were partially obtained with radiopharmaceuticals other than ^{177}Lu-DOTA ligands, AAs are most commonly used in PRRT (*12*).

Para-aminohippurate, also known as *p*-aminohippuric acid (PAH), is an anionic substrate and is frequently used to assess renal plasma flow and glomerular filtration rate (GFR) (*13*,*14*). Maeda et al. (*15*) reported a surprising increase in the clearance of benzylpenicillin when coadministered with PAH, suggesting a potential inhibition of renal reabsorption processes. In addition, PAH is a substrate for organic anion transmembrane transporters (OAT1, OAT2, and OAT4) that are indicated to be involved in renal clearance of somatostatin analogs (*16*,*17*). It was specifically shown that PAH comedication reduces kidney uptake of small peptide radiopharmaceuticals (*18*). Because of shorter infusion

Received Sep. 5, 2023; revision accepted Mar. 4, 2024.
For correspondence or reprints, contact Alexandros Moraitis (alexandros.moraitis@uk-essen.de).
Published online Apr. 18, 2024.

times for PAH than for AA and a possible reduction of side effects reported with AA, such as nausea and hyperkalemia (*10*), administration of PAH in the clinical setting during PRRT might further improve patient throughput and tolerance to PRRT.

In this study, we investigated the safety and efficacy of PAH coinfusion during ^{177}Lu-DOTATOC treatment in patients with gastroenteropancreatic NETs in comparison to our current standard protocol of AA infusion.

MATERIALS AND METHODS

Preliminary Preclinical Biodistribution Study

A study was performed before clinical investigations in healthy male Wistar rats to assess the biodistribution profile of ^{177}Lu-DOTATOC when administered along with PAH. Before intravenous injection of a mean ± SD of 0.9 ± 0.1 MBq of ^{177}Lu-DOTATOC, rats (n = 8–10 per group) were injected intraperitoneally with 1 mL of saline solution (0.9% sodium chloride [NaCl]), AA solution containing arginine and lysine (200 mg/mL), or PAH solution (200 mg/mL). Subsequently, the rats were sacrificed 5 or 60 min after injection of ^{177}Lu-DOTATOC, and kidney activity was measured in a calibrated well counter. For each of the 3 coinfusion groups, 4–5 kidney uptake values were available at each time point after injection. The experiments were conducted by Helmholtz-Zentrum Dresden-Rossendorf on behalf of ITM Medical Isotopes Garching GmbH according to the German Animal Welfare Act and European Union directive 2010/63/EU on the protection of animals used for scientific purposes and were approved by the provincial headquarters in Dresden (protocol DD24.1-5131/450/16).

Clinical Application

Since it became available at our department (Department of Nuclear Medicine at the University Hospital in Essen, Germany), PAH has been offered alternatively to AA infusion in PRRT of patients with metastatic or unresectable gastroenteropancreatic NETs. Data of the first patients receiving PAH were analyzed retrospectively. The primary aims of the study were to assess the clinical safety of PAH and to evaluate kidney and bone marrow dosimetry of PAH coinfusion during ^{177}Lu-DOTATOC treatment. The secondary aim was to compare the findings with that of the established coinfusion of AA. All patients provided written informed consent for clinical PAH application and PRRT. The local ethics committee (University of Duisburg-Essen Medical Faculty, protocol 23-11120-BO) approved the study and waived the need for study-specific consent.

Patients and Drug Administration

Fourteen gastroenteropancreatic NET patients treated between November 2021 and November 2022 who received PAH for renal protection were initially identified. Of those, 2 patients were excluded because of disease progression after the first cycle and were not further evaluated. In addition to international joint recommendations on patient eligibility for ^{177}Lu-DOTATOC treatment (*19*), patients were offered PRRT only if they were at least 18 y of age and they had an initial GFR of at least 50 mL/min. All patients showed somatostatin receptor–positive lesions confirmed by ^{68}Ga-DOTATOC PET/CT imaging. Patient characteristics are summarized in Table 1.

Patients were administered 3 cycles of 7.4 GBq of ^{177}Lu-DOTATOC each, injected intravenously in 30–45 min via automated infusion pumps and accompanied by 500 mL of 0.9% NaCl solution. Concomitantly, either PAH or AA solution was infused for renal protection via separate tubing. A PAH amount of approximately 8 g was used, resulting in a total infusion volume of less than 100 mL (*20*). More specifically, a priming rate of 160 mg of PAH per minute for 16 min, followed by a maintenance rate of 110 mg/min for 48 min, was used to reach an estimated steady-state PAH plasma concentration of 450 mg/L (total infusion time of approximately 70 min). A detailed description of PAH pharmacokinetic assumptions used for the calculation of PAH plasma concentration is provided in supplemental materials (supplemental materials are available at http://jnm.snmjournals.org). The AA solution contained positively charged lysine and arginine (each 25 g) and was infused in 2 L of NaCl solution over 4 h (*5*).

TABLE 1
Patient Characteristics at Time of First Treatment Cycle

Patient	Sex	Age (y)	Height (cm)	Weight (kg)	Protectant at 1 cycle	Type of NET	DD (mo)	Previous therapy	Prior cum. PRRT activity (GBq)
1	M	46	181	86	PAH	Intestinal	28	S, PRRT	51.6
2	M	31	178	69	PAH	Rectal	8	CT, PRRT	22.6
3	M	50	178	88	PAH	Intestinal	162	S, CT, SIRT, PRRT	44.6
4	F	55	160	76	PAH	Intestinal	81	S, PRRT	49.5
5	M	48	181	65	PAH	Intestinal	17	S, PRRT	22.0
6	F	67	175	61	PAH	Intestinal	212	S, PRRT	66.3
7	M	52	174	69	AA	Intestinal	16	PRRT	15.1
8	M	78	192	85	AA	CUP	65	S, PRRT	15.3
9	F	77	160	49	AA	Intestinal	107	S, PRRT	22.7
10	F	84	170	67	AA	Intestinal	71	PRRT	52.3
11	M	61	177	78	AA	Intestinal	50	None	0
12	M	63	175	79	AA	Pancreatic	29	CT	0

DD = disease duration; cum. = cumulative; S = surgery; CT = chemotherapy; SIRT = selective internal radiotherapy; CUP = cancer of unknown primary.

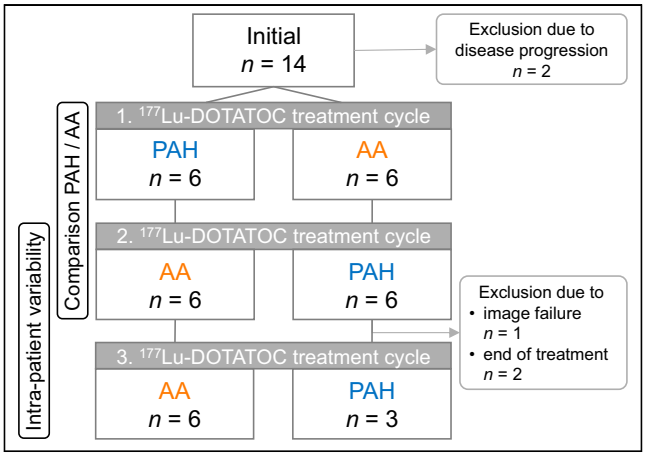

FIGURE 1. Administration flowchart.

The administration flowchart in Figure 1 illustrates the choice of renal protectant during the course of 3 treatment cycles. Of the 12 patients who were evaluated, 6 received PAH in the first cycle, followed by AA in the second cycle. The other 6 patients received the renal protectants in opposite order. The third treatment cycle was given with coinfusion of the same renal protectant as used in the second cycle to assess intrapatient variability of dosimetry calculations. For 3 patients, dosimetry data were not available for the third cycle because of imaging failure ($n = 1$) or end of treatment ($n = 2$).

Data Collection: Imaging, Blood Sampling, and Laboratory Data

The hybrid approach was used for dosimetry imaging consisting of whole-body planar imaging at 1, 24, and 48 h and 1 SPECT/CT scan 48 h after administration covering the abdomen. All scans were performed on a Symbia Intevo T2 (Siemens Healthineers) SPECT/CT system equipped with a medium-energy collimator. For anterior and posterior whole-body planar images, the peak energy window was centered at 208 keV (width, ±7.5%) and the lower and upper energy windows for scatter correction were ±5%. Images were acquired with a scan velocity of 10 cm/min in a 256 × 1,024 matrix. Each patient was scanned along with an individually prepared ^{177}Lu reference standard placed between the heels to monitor system stability. Acquisition parameters used in the SPECT/CT scans were a 208-keV energy peak (width, ±7.5%), upper and lower scatter window widths of ±5% each, 3° angular step size, 60 projections, and 20 s per projection. Standard attenuation and scatter correction were applied to reconstruct images into a 128 × 128 transverse matrix with cubical voxels of a 4.8-mm side length using an ordered-subset conjugate gradient maximization algorithm with 48 iterations, 1 subset, and no gaussian filter (xQuant; Siemens Healthineers) to provide fully quantitative images (*21*).

Venous blood samples were drawn before treatment and at 5 min, 30 min, and 2, 4, 24, and 48 h after the end of ^{177}Lu-DOTATOC infusion. Blood activity in each sample was measured in a calibrated well counter (Wizard^2 2480 3"; PerkinElmer). The activity values were corrected for detector dead time, filling level, and decay to the time of administration. Sample volumes were determined gravimetrically to obtain the blood activity concentration.

Safety was assessed by monitoring clinical laboratory parameters including hematologic data (hemoglobin, red blood cell counts, white blood cell counts, and platelet counts), renal parameters (creatinine level and estimated GFR), and electrolytes (sodium, potassium, chloride, phosphate, and calcium). These were obtained before and 24 h after treatment.

Radiation Dosimetry

Kidney and Bone Marrow Time–Activity Curves. For the kidneys, manual volume segmentation was performed for the first cycle on low-dose CT images. The volumes of interest were propagated into other cycles. The imaged SPECT/CT activity concentration of each kidney was corrected individually for the partial-volume effect by applying experimentally derived recovery coefficients (*21*). In planar imaging, background and attenuation-corrected geometric mean values from anterior and posterior counts were calculated using the conjugate view method with additional self-attenuation within the kidney, as proposed by the MIRD committee (*22*). The resulting count value from the 48-h planar images was scaled to equal the partial-volume effect–corrected activity from SPECT/CT. Subsequently, the same scaling factor was applied to the count values from the 1- and 24-h planar images to construct the time–activity curve for each kidney.

Bone marrow activity was estimated using the blood method (*23*), assuming that the activity concentration in the bone marrow was equal to that in the blood (*24*). To obtain the bone marrow activity, the blood activity concentration from each blood sample was multiplied by the respective male or female reference bone marrow mass and scaled by the ratio of individual-to-reference patient mass (*25*). To account for cross-radiation from the remainder of the body, whole-body retention curves were constructed from planar images by normalizing the geometric mean count values of the whole body to the geometric mean value from the first measurement (1 h after injection). Patients were asked not to void until the first imaging time point to preserve translation from counts to activity. Alternatively, the excreted urine was collected and scanned along with the patient.

Time-Integrated Activity Coefficients (TIACs) and Absorbed Dose Coefficients. After normalizing kidney and bone marrow time–activity curves to the administered activities, the resulting uptake curves and whole-body retention curves were used to calculate the TIACs. Point-to-point effective half-lives were derived by calculating monoexponential functions between adjacent time points for each kidney, the bone marrow, and the whole body. TIACs were obtained by integrating the point-to-point monoexponential functions (*26*). For the kidneys and bone marrow, the effective half-life between 1 and 24 h after administration was used to extrapolate to the end of infusion ($t = 0$). For the kidneys, an effective half-life of 50 h was assumed for integration after the last (48 h) time point (*27*,*28*), whereas for bone marrow and whole-body TIACs, the effective half-life between 24 and 48 h was used.

Dosimetry estimations were performed using the MIRD concept. The left and right kidneys were summarized into a single source organ of renal tissue, and absorbed dose coefficients were calculated individually using OLINDA/EXM 2.2 software. The bone marrow–absorbed dose was calculated as proposed by Traino et al. (*29*) to account for patient-specific S value scaling based on the individual's whole-body and bone marrow mass.

Software and Statistics

Image analysis was performed using PMOD version 4.2 software (PMOD Technologies Ltd.). Statistical analysis, performed using GraphPad Prism version 5.03 (GraphPad Software Inc.), included calculation of mean and median values and the measure of dispersion expressed as SD and interquartiles. Spearman correlation analysis and the Mann–Whitney U test were used, and significance was assumed for a P value of no more than 0.05.

RESULTS

Preliminary Preclinical Biodistribution Study

Kidney uptake in healthy male Wistar rats, expressed as the percentage of injected activity per gram of renal tissue, is shown in

Supplemental Figure 1. In evaluations of both 5 and 60 min after ^{177}Lu-DOTATOC injection, PAH significantly decreased the radioactivity in the kidneys from that occurring with NaCl solution. Elimination of ^{177}Lu-DOTATOC was also significantly faster with AA than with NaCl solution. No signs of acute and delayed toxicity were observed with the protective agents.

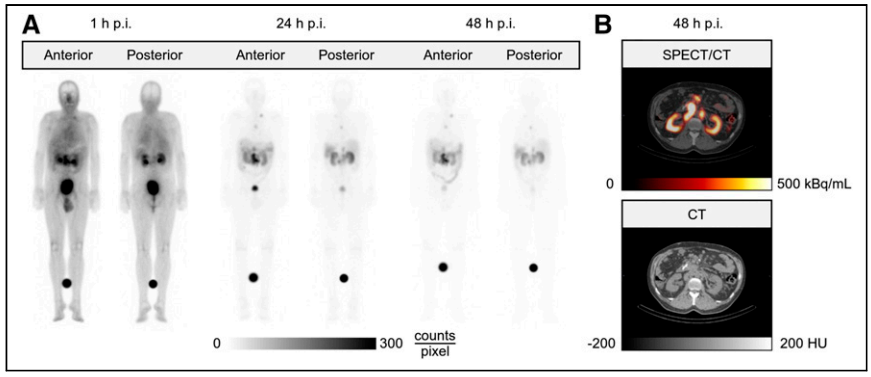

FIGURE 2. Sequential planar images (A) and 1 fused axial SPECT/CT and corresponding CT slice (B) of representative patient (patient 11, cycle 2) after PAH coinfusion during ^{177}Lu-DOTATOC treatment. HU = Hounsfield units; p.i. = postinjection.

Patients

Twelve patients, treated in 33 individual PRRT cycles, were administered a mean ± SD of 7.5 ± 0.2 GBq of ^{177}Lu-DOTATOC per cycle. In 15 cycles, PAH was coinfused for renal protection (AA was coinfused in 18 cycles). The mean time between subsequent cycles was 57 ± 12 d. The actual imaging time points after administration were 1 ± 1, 20 ± 2, and 43 ± 2 h for planar imaging and 44 ± 2 h for SPECT/CT.

Safety

No grade 3 or 4 adverse events, according to the Common Terminology Criteria for Adverse Events, were reported with either PAH or AA. No significant changes in mean serum creatinine, GFR, or serum electrolytes (sodium, potassium, chloride, phosphate, and calcium) were observed before or 24 h after treatment under PAH ($P \geq 0.20$). Under AA, serum chloride and serum phosphate increased significantly after treatment (105.8 vs. 107.8 mmol/L, $P < 0.01$, and 3.13 vs. 3.80 mg/dL, $P < 0.01$, respectively). One patient per renal protectant (patient 9 under PAH and patient 1 under AA) showed a grade 1 creatinine increase with a correlated grade 2 GFR decrease, and 1 patient (patient 6) showed grade 1 hyperkalemia under AA. Based on hematologic parameters measured before treatment of cycle 1 and then cycle 2, 2 PAH patients (patients 4 and 5) developed grade 1 anemia and 1 AA patient (patient 10) developed grade 2 anemia. One PAH patient (patient 3) showed grade 1 leukopenia and thrombocytopenia. No other adverse events were reported.

Radiation Dosimetry

Figure 2 shows planar and SPECT/CT images of a representative patient after PAH coinfusion during PRRT (patient 11, cycle 2).

TABLE 2
Kidney– and Bone Marrow–Absorbed Dose Coefficients Under Coinfusion of Either PAH or AA During ^{177}Lu-DOTATOC Treatment

	Kidney–absorbed dose coefficient (Gy/GBq)			Bone marrow–absorbed dose coefficient (Gy/GBq)		
Patient	PAH	AA	%-Δ	PAH	AA	%-Δ
1	0.43	0.34	26	0.008	0.007	14
2	0.35	0.44	−20	0.017	0.017	0
3	0.83	0.65	28	0.009	0.009	0
4	0.74	0.78	−5.1	0.009	0.010	−10
5	0.73	0.83	−12	0.010	0.012	−17
6	0.60	0.44	36	0.011	0.010	10
7	0.73	0.50	46	0.011	0.010	10
8	0.46	0.39	18	0.009	0.010	−10
9	0.52	0.67	−22	0.021	0.019	11
10	0.53	0.40	33	0.014	0.012	17
11	0.66	0.42	57	0.011	0.010	10
12	0.62	0.49	27	0.018	0.016	13
Mean	0.60	0.53		0.012	0.012	
SD	0.14	0.16		0.004	0.003	
Median	0.61	0.47		0.011	0.010	
Min	0.35	0.34		0.008	0.007	
Max	0.83	0.83		0.021	0.019	

%-Δ = intrapatient percentage difference from PAH to AA; Min = minimum; Max = maximum.

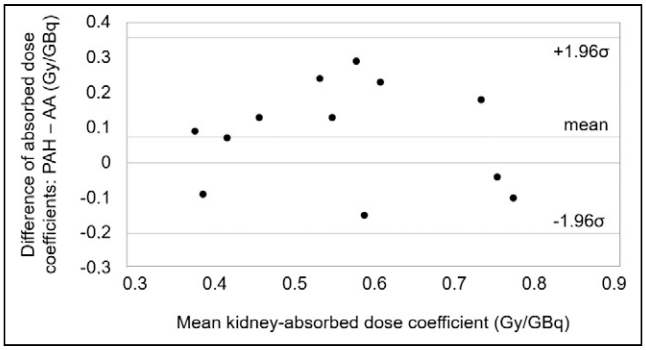

FIGURE 3. Bland–Altman plot of kidney–absorbed dose coefficients during ^{177}Lu-DOTATOC treatment with coinfusion of either PAH or AA.

Time–activity curves of the left and right kidneys are provided in Supplemental Figure 2. Kidney, bone marrow, and whole-body TIACs with coinfusion of PAH and AA are provided in Supplemental Tables 1–3.

For the kidneys, intrapatient variability, expressed as mean ± SD absolute percentage deviation of absorbed dose coefficients from cycle 3 to cycle 2 (where the same renal protectant was used), was 17.6% ± 9.9% (Supplemental Table 4). Kidney–absorbed dose coefficients of cycles 1 and 2, used to compare PAH and AA, are listed in Table 2 and illustrated by the Bland–Altman plot in Figure 3. The mean kidney–absorbed dose coefficient was higher for PAH by 0.07 Gy/GBq yet not significant (P = 0.14). The highest single value of 0.83 Gy/GBq was observed with both AA (patient 5) and PAH (patient 3). The largest difference in a patient using different renal protectants was observed in patient 11 (0.66 Gy/GBq with PAH vs. 0.42 Gy/GBq with AA). In Figure 4, kidney–absorbed dose coefficients are plotted against the percentage of kidney uptake at 48 h after administration (Fig. 4A) and total kidney volume (Fig. 4B). For both PAH and AA, absorbed dose to the kidneys correlated with the 48-h uptake (ρ = 0.8). No correlation was found between kidney–absorbed dose coefficients and total kidney volume (ρ = −0.1). Based on extrapolated cumulative kidney-absorbed doses for 4 cycles (assuming 7.4 GBq per cycle), 1 patient with AA and 1 patient with PAH (8% of our patient group) would exceed the 23-Gy toxicity threshold. For at least 50% of patients (6 patients for PAH and 8 patients for AA), 5 treatment cycles would have been feasible before reaching the toxicity threshold.

For bone marrow, intrapatient variability was 6.4% ± 3.9% (Supplemental Table 4). Mean ± SD bone marrow–absorbed dose coefficients were 0.012 ± 0.004 Gy/GBq with PAH and 0.012 ± 0.003 Gy/GBq with AA (Table 2). Extrapolation (4 cycles, 7.4 GBq each) of the highest single value for each PAH and AA patient would yield a cumulative bone marrow–absorbed dose of approximately 0.6 Gy (below the 2-Gy toxicity threshold for bone marrow).

DISCUSSION

This study is the first, to our knowledge, to report the safety and efficacy of PAH coinfusion in patients with gastroenteropancreatic NETs undergoing ^{177}Lu-DOTATOC PRRT. In our cohort, dosimetry revealed a comparable nephroprotective effect of PAH and

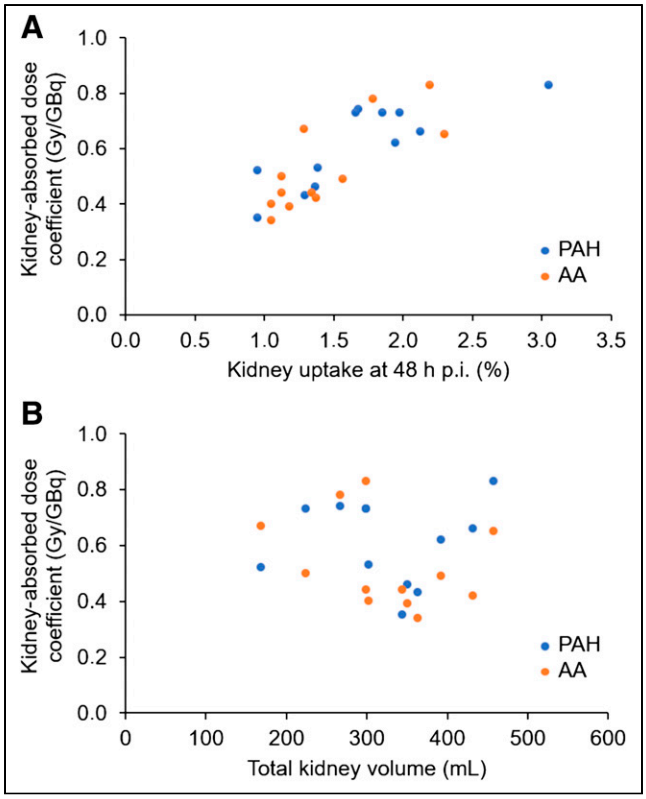

FIGURE 4. (A) Kidney–absorbed dose coefficient dependence on kidney percentage uptake 48 h after administration (ρ = 0.80). (B) No correlation was found between kidney–absorbed dose coefficients and total kidney volume (ρ = −0.10). p.i. = postinfusion.

AA coinfusion in terms of compliance with toxicity thresholds. In addition, PAH was well tolerated and improved patient comfort during treatment because of shorter infusion times and possible reduction of hyperkalemia.

One of the first clinical experiences with ^{90}Y-DOTATOC, performed by Otte et al. (*30*), had already identified the need to reduce renal toxicity by improving inhibition of renal uptake during PRRT. Later, Rolleman et al. (*10*) investigated the nephroprotective effect of different AA solutions and concluded that a mixture of 25 g of lysine and 25 g of arginine provides the optimal trade-off between protection and AA-induced side effects, such as vomiting and hyperkalemia. Despite its known side effects, this AA solution is considered the current standard for renal protection in PRRT (*12*,*19*). In addition, Puszkiel et al. (*31*) evaluated the impact of AA coinfusion on ^{177}Lu-DOTATATE excretion kinetics in patients with gastroenteropancreatic NETs and observed large interpatient variability. Promising alternatives to overcome these effects are under investigation (*32*,*33*). In the present study, PAH coinfusion showed no increase in mean serum potassium; however, an increase was observed with AA, revealing a potential reduction of hyperkalemia-related morbidities.

For PAH to develop a nephroprotective effect in this study, saturation of the secretory capacity in proximal tubular cells was desired. To saturate the tubular secretory capacity, Dowling et al. (*20*) used PAH plasma concentrations of more than 800 mg/L, which were well tolerated, except for a few subjects reporting a

slight warming sensation at the highest priming rate (200 mg/min), which ceased within 5–10 min after administration. To avoid these side effects, 80% of this rate (160 mg/min) was used in this study. In addition, we aimed at a PAH plasma concentration of 450 mg/L, which according to Dowling et al. (*20*) corresponded to an approximate saturation of 80% of the secretory capacity.

Mean kidney-absorbed doses under PAH were 0.60 Gy/GBq compared with 0.53 Gy/GBq under AA, and the protectants showed equal nephroprotective capabilities in terms of compliance with the 23-Gy toxicity threshold for extrapolated cumulative kidney-absorbed doses (1 exceedance per renal protectant). In general, the applicability of this absorbed dose limit is questioned as being adopted from external beam radiation (*34*). Because of the lower absorbed dose rates in PRRT, the absorbed dose limit for kidney toxicity may be higher than 23 Gy. Bodei et al. (*35*) showed that a safe renal–absorbed dose limit might be a biologic effective dose of up to 40 Gy in patients without risk factors and 28 Gy in patients with certain risk factors in ^{90}Y-PRRT. Because of its nonuniform irradiation compared with ^{90}Y, application of ^{177}Lu-PRRT is expected to allow for even higher dosimetry constraints (*36*). When multiplying our extrapolated kidney-absorbed doses by 1.09—the dose–to–biologic effective dose conversion factor for PRRT suggested by Sundlöv et al. (*36*)—no patient would have exceeded the conservative 28-Gy biologic effective dose threshold, which is in line with our clinical observations.

Bone marrow–absorbed dose coefficients were equal under coinfusion of PAH and AA, with no value greater than 0.021 Gy/GBq. In extensively treated patients, hematologic toxicities might become relevant dose-limiting factors. Promising activity escalation strategies, such as the P-PRRT trial, could achieve response rates of 59% at the cost of subacute grade 3 or 4 lymphocytopenia in 52% of patients (*37*). In addition, Schäfer et al. (*38*) recently reported 3 cases of radiation nephropathy induced by renal thrombotic microangiopathy in the context of extensively treated ^{177}Lu-PSMA patients. Hence, the use of effective renal protectants should also aim at preserving kidney functions to allow faster excretion of radioactive compounds and therefore reduce systemic radiation exposure.

It was established that the renal retention of the 8-AA peptide DOTATOC primarily resulted from megalin and cubilin endocytosis, followed by transportation for protein degradation in the lysosome (*5*). However, larger proteins such as albumin (65–70 kDa) typically undergo tubular reabsorption mechanisms (*39*). The structurally similar compound ^{177}Lu-oxodotreotide (DOTATATE) was reported to exhibit excretion with a radiochemical purity close to 100% within the initial 48 h, indicating the absence of further lysosomal degradation. In addition, probenecid—an inhibitor targeting transporters similar to PAH—was shown preclinically to influence kidney retention of ^{111}In-DOTATOC (*16*). Our investigations expand on these findings, suggesting that transporters other than megalin and cubilin may also play a significant role in the renal excretion or reabsorption of DOTATOC. Several transporters located on the apical side of proximal tubular cells and the cortical collecting duct, such as OATK1, OAT-K2, OAT polypeptide 1, multidrug-resistance-associated protein 2, and sodium-dependent inorganic phosphate transporter, serve as substrates for PAH, and their role in the excretion of peptides or xenobiotics remains incompletely understood (*40*). The presented study did not delve into mechanistic details, and the explanations provided remain speculative. Further biologic studies are warranted to explore these aspects in greater depth.

The study was mainly limited by its small number of patients and patient heterogeneity with respect to their treatment history (Table 1), which could have influenced the nephroprotective effect of PAH and AA. Both protectants need to be evaluated for PRRT-naïve patients. In addition, dosimetry estimations were limited to the 48-h imaging time point. A later imaging time point would have enabled the assessment of late-phase kidney kinetics to reduce the impact of fit functions after the last imaging time point. Lastly, direct assessment of the PAH blood–plasma concentration would provide more accurate insight into individual PAH clearance to help optimize PAH dosing. These data were not available for this retrospective analysis.

CONCLUSION

Nephroprotection of PAH coinfusion during ^{177}Lu-DOTATOC PRRT was comparable to that of AA in terms of compliance with renal toxicity thresholds. It was well tolerated and may improve patient quality of life during treatment by potentially reducing hyperkalemia and nausea. In addition, implementation of PAH in treatment protocols might enhance patient tolerance to PRRT because of shorter infusion times. Further research is required to investigate the safety profile at varying PAH plasma concentrations.

DISCLOSURE

Walter Jentzen received research funding from Siemens Healthineers. Ken Herrmann reports personal fees from Bayer, SIRTEX, Adacap, Curium, Endocyte, IPSEN, Siemens Healthineers, GE Healthcare, Amgen, Novartis, Y-mAbs, Aktis Oncology, Theragnostics, Pharma15, Debiopharm, AstraZeneca, and Janssen; personal fees and other support from Sofie Biosciences; nonfinancial support from ABX; and grants and personal fees from BTG outside of the submitted work. Wolfgang Fendler reports fees from Sofie Biosciences (research funding), Janssen (consultant and speaker), Calyx (consultant and image review), Bayer (consultant, speaker, and research funding), and Novartis, Telix, GE, and Eczacıbaşı Monrol (speaker) outside of the submitted work. David Kersting reports support from the Universitätsmedizin Essen Clinician Scientist Academy and the German Research Foundation (DFG) under grant FU356/12-2, further support by the DFG, and a research grant from Pfizer outside of the submitted work. Marian Meckel, with ITM, declares patent interests related to the use of PAH as a renal protectant presented in this article. No other potential conflict of interest relevant to this article was reported.

ACKNOWLEDGMENTS

We express our gratitude to Prof. Dr. Thomas C. Dowling for his efforts to provide us with historical data, which were essential to validate our PAH pharmacokinetic model. ITM, through Marian Meckel, also acknowledges the contribution of Domokos Mathe and Ralf Bergmann for the animal handling and experiments.

KEY POINTS

QUESTION: Is PAH coinfusion for renal protection effective and safe in patients with NETs undergoing PRRT?

PERTINENT FINDINGS: PAH was well tolerated and improved patient comfort during treatment because of shorter infusion times and the potential reduction of hyperkalemia and nausea. In our cohort, dosimetry revealed a comparable nephroprotective effect between PAH and AA coinfusion in terms of compliance with toxicity thresholds.

IMPLICATIONS FOR PATIENT CARE: Implementation of PAH coinfusion in treatment protocols may enhance patient tolerance to PRRT and increase patient throughput.

REFERENCES

1. Kwekkeboom DJ, de Herder WW, Kam BL, et al. Treatment with the radiolabeled somatostatin analog [^{177}Lu-DOTA^{0},Tyr^{3}]octreotate: toxicity, efficacy, and survival. *J Clin Oncol.* 2008;26:2124–2130.
2. Strosberg J, El-Haddad G, Wolin E, et al. Phase 3 trial of ^{177}Lu-DOTATATE for midgut neuroendocrine tumors. *N Engl J Med.* 2017;376:125–135.
3. Sabet A, Ezziddin K, Pape UF, et al. Long-term hematotoxicity after peptide receptor radionuclide therapy with ^{177}Lu-octreotate. *J Nucl Med.* 2013;54:1857–1861.
4. Garkavij M, Nickel M, Sjögreen-Gleisner K, et al. ^{177}Lu-[DOTA^{0},Tyr^{3}] octreotate therapy in patients with disseminated neuroendocrine tumors: analysis of dosimetry with impact on future therapeutic strategy. *Cancer.* 2010;116:1084–1092.
5. Rolleman EJ, Melis M, Valkema R, Boerman OC, Krenning EP, de Jong M. Kidney protection during peptide receptor radionuclide therapy with somatostatin analogues. *Eur J Nucl Med Mol Imaging.* 2010;37:1018–1031.
6. Svensson J, Berg G, Wängberg B, Larsson M, Forssell-Aronsson E, Bernhardt P. Renal function affects absorbed dose to the kidneys and haematological toxicity during ^{177}Lu-DOTATATE treatment. *Eur J Nucl Med Mol Imaging.* 2015; 42:947–955.
7. Vegt E, van Eerd JE, Eek A, et al. Reducing renal uptake of radiolabeled peptides using albumin fragments. *J Nucl Med.* 2008;49:1506–1511.
8. Jamar F, Barone R, Mathieu I, et al. ^{86}Y-DOTA^{0}-D-Phe1-Tyr^{3}-octreotide (SMT487): a phase 1 clinical study—pharmacokinetics, biodistribution and renal protective effect of different regimens of amino acid co-infusion. *Eur J Nucl Med Mol Imaging.* 2003;30:510–518.
9. Vegt E, Wetzels JF, Russel FG, et al. Renal uptake of radiolabeled octreotide in human subjects is efficiently inhibited by succinylated gelatin. *J Nucl Med.* 2006; 47:432–436.
10. Rolleman EJ, Valkema R, de Jong M, Kooij PP, Krenning EP. Safe and effective inhibition of renal uptake of radiolabelled octreotide by a combination of lysine and arginine. *Eur J Nucl Med Mol Imaging.* 2003;30:9–15.
11. Bodei L, Cremonesi M, Zoboli S, et al. Receptor-mediated radionuclide therapy with ^{90}Y-DOTATOC in association with amino acid infusion: a phase I study. *Eur J Nucl Med Mol Imaging.* 2003;30:207–216.
12. Hope TA, Lisa B, Jennifer AC, et al. NANETS/SNMMI consensus statement on patient selection and appropriate use of ^{177}Lu-DOTATATE peptide receptor radionuclide therapy. *J Nucl Med.* 2020;61:222–227.
13. Chasis H, Redish J, Goldring W, Ranges HA, Smith HW. The use of sodium *p*-aminohippurate for the functional evaluation of the human kidney. *J Clin Invest.* 1945;24:583–588.
14. Smith HW, Finkelstein N, Aliminosa L, Crawford B, Graber M. The renal clearances of substituted hippuric acid derivatives and other aromatic acids in dog and man. *J Clin Invest.* 1945;24:388–404.
15. Maeda K, Tian Y, Fujita T, et al. Inhibitory effects of *p*-aminohippurate and probenecid on the renal clearance of adefovir and benzylpenicillin as probe drugs for organic anion transporter (OAT) 1 and OAT3 in humans. *Eur J Pharm Sci.* 2014; 59:94–103.
16. Stahl AR, Wagner B, Poethko T, et al. Renal accumulation of [^{111}In]DOTATOC in rats: influence of inhibitors of the organic ion transport and diuretics. *Eur J Nucl Med Mol Imaging.* 2007;34:2129–2134.
17. Sweet DH, Wolff NA, Pritchard JB. Expression cloning and characterization of ROAT1: the basolateral organic anion transporter in rat kidney. *J Biol Chem.* 1997; 272:30088–30095.
18. Meckel M, Osl T, Zhernosekov K, inventors. ITM Isotopen Technologien München AG, assignee. Para-aminohippuric acid (PAH) as a renal protective substance. Patents WO2020224780A1, PCT/EP2019/061882. November 12, 2020.
19. Bodei L, Mueller-Brand J, Baum RP, et al. The joint IAEA, EANM, and SNMMI practical guidance on peptide receptor radionuclide therapy (PRRNT) in neuroendocrine tumours. *Eur J Nucl Med Mol Imaging.* 2013;40:800–816.
20. Dowling TC, Frye RF, Fraley DS, Matzke GR. Characterization of tubular functional capacity in humans using para-aminohippurate and famotidine. *Kidney Int.* 2001;59:295–303.
21. Dickson JC, Armstrong IS, Gabina PM, et al. EANM practice guideline for quantitative SPECT-CT. *Eur J Nucl Med Mol Imaging.* 2023;50:980–995.
22. Siegel JA, Thomas SR, Stubbs JB, et al. MIRD pamphlet no. 16: techniques for quantitative radiopharmaceutical biodistribution data acquisition and analysis for use in human radiation dose estimates. *J Nucl Med.* 1999;40:37–61.
23. Sgouros G. Bone marrow dosimetry for radioimmunotherapy: theoretical considerations. *J Nucl Med.* 1993;34:689–694.
24. Forrer F, Krenning EP, Kooij PP, et al. Bone marrow dosimetry in peptide receptor radionuclide therapy with [^{177}Lu-DOTA^{0},Tyr^{3}]octreotate. *Eur J Nucl Med Mol Imaging.* 2009;36:1138–1146.
25. ICRP. Basic anatomical and physiological data for use in radiological protection reference values: ICRP publication 89. *Ann ICRP.* 2002;32:5–265.
26. Jentzen W, Freudenberg L, Eising EG, Sonnenschein W, Knust J, Bockisch A. Optimized ^{124}I PET dosimetry protocol for radioiodine therapy of differentiated thyroid cancer. *J Nucl Med.* 2008;49:1017–1023.
27. Hänscheid H, Lapa C, Buck AK, Lassmann M, Werner RA. Dose mapping after endoradiotherapy with ^{177}Lu-DOTATATE/DOTATOC by a single measurement after 4 days. *J Nucl Med.* 2018;59:75–81.
28. Hänscheid H, Lapa C, Buck AK, Lassmann M, Werner RA. Absorbed dose estimates from a single measurement one to three days after the administration of ^{177}Lu-DOTATATE/-TOC. *Nuklearmedizin.* 2017;56:219–224.
29. Traino AC, Ferrari M, Cremonesi M, Stabin MG. Influence of total-body mass on the scaling of S-factors for patient-specific, blood-based red-marrow dosimetry. *Phys Med Biol.* 2007;52:5231–5248.
30. Otte A, Herrmann R, Heppeler A, et al. Yttrium-90 DOTATOC: first clinical results. *Eur J Nucl Med.* 1999;26:1439–1447.
31. Puszkiel A, Bauriaud-Mallet M, Bourgeois R, Dierickx L, Courbon F, Chatelut E. Evaluation of the interaction of amino acid infusion on ^{177}Lu-DOTATATE pharmacokinetics in patients with gastroenteropancreatic neuroendocrine tumors. *Clin Pharmacokinet.* 2019;58:213–222.
32. Courault P, Deville A, Habouzit V, et al. Amino acid solutions for ^{177}Lu-oxodotreotide premedication: a tolerance study. *Cancers (Basel).* 2022;14:5212.
33. Lambert M, Dierickx L, Brillouet S, Courbon F, Chatelut E. Comparison of two types of amino acid solutions on ^{177}Lu-DOTATATE pharmacokinetics and pharmacodynamics in patients with metastatic gastroenteropancreatic neuroendocrine tumors. *Curr Radiopharm.* 2022;15:164–172.
34. Strigari L, Benassi M, Chiesa C, Cremonesi M, Bodei L, D'Andrea M. Dosimetry in nuclear medicine therapy: radiobiology application and results. *Q J Nucl Med Mol Imaging.* 2011;55:205–221.
35. Bodei L, Cremonesi M, Ferrari M, et al. Long-term evaluation of renal toxicity after peptide receptor radionuclide therapy with ^{90}Y-DOTATOC and ^{177}Lu-DOTATATE: the role of associated risk factors. *Eur J Nucl Med Mol Imaging.* 2008;35:1847–1856.
36. Sundlöv A, Sjögreen-Gleisner K, Svensson J, et al. Individualised ^{177}Lu-DOTATATE treatment of neuroendocrine tumours based on kidney dosimetry. *Eur J Nucl Med Mol Imaging.* 2017;44:1480–1489.
37. Del Prete M, Buteau FA, Arsenault F, et al. Personalized ^{177}Lu-octreotate peptide receptor radionuclide therapy of neuroendocrine tumours: initial results from the P-PRRT trial. *Eur J Nucl Med Mol Imaging.* 2019;46:728–742.
38. Schäfer H, Mayr S, Büttner-Herold M, et al. Extensive ^{177}Lu-PSMA radioligand therapy can lead to radiation nephropathy with a renal thrombotic microangiopathy-like picture. *Eur Urol.* 2023;83:385–390.
39. Tojo A, Kinugasa S. Mechanisms of glomerular albumin filtration and tubular reabsorption. *Int J Nephrol.* 2012;2012:481520.
40. Sekine T, Miyazaki H, Endou H. Molecular physiology of renal organic anion transporters. *Am J Physiol Renal Physiol.* 2006;290:F251–F261.